Locating the QCD critical end point through peaked baryon number susceptibilities along the freeze-out line*

Zhibin Li(李志镔)[1,2;1)] Yidian Chen(陈亦点)[1,2;2)] Danning Li(李丹凝)[3;3)] Mei Huang(黄梅)[1,2,4;4)]

[1] Institute of High Energy Physics, Chinese Academy of Sciences, Beijing 100049, China
[2] School of Physics Sciences, University of Chinese Academy of Sciences, Beijing 100049, China
[3] Department of Physics, Jinan University, Guangzhou 510632, China
[4] Theoretical Physics Center for Science Facilities, Chinese Academy of Sciences, Beijing 100049, China

Abstract: We investigate the baryon number susceptibilities up to fourth order along different freeze-out lines in a holographic QCD model with a critical end point (CEP), and we propose that the peaked baryon number susceptibilities along the freeze-out line can be used as a clean signature to locate the CEP in the QCD phase diagram. On the temperature and baryon chemical potential plane, the cumulant ratio of the baryon number susceptibilities (up to fourth order) forms a ridge along the phase boundary, and develops a sword-shaped "mountain" standing upright around the CEP in a narrow and oblate region. The measurement of baryon number susceptibilities from heavy-ion collision experiments is along the freeze-out line. If the freeze-out line crosses the foot of the CEP mountain, then one can observe the peaked baryon number susceptibilities along the freeze-out line, and the kurtosis of the baryon number distributions has the highest magnitude. The data from the first phase of the beam energy scan program at the Relativistic Heavy Ion Collider indicates that there should be a peak of the kurtosis of the baryon number distribution at a collision energy of around 5 GeV, which suggests that the freeze-out line crosses the foot of the CEP mountain and the summit of the CEP should be located nearby, around a collision energy of 3–7 GeV.

Keywords: QCD, baryon number susceptibilities, critical end point, phase transition

PACS: 12.38.Mh, 25.75.Nq, 11.10.Wx **DOI:** 10.1088/1674-1137/42/1/013103

1 Introduction

Quantum chromodynamics (QCD) is the fundamental theory of the strong interaction. The QCD vacuum structure and its phase diagram under extreme conditions has been always one of the most attractive topics to understand the nonperturbative nature of the strong interaction. In the QCD vacuum, chiral symmetry is spontaneously broken and color-charged quarks and gluons are confined. It is expected that at high temperature and/or baryon density, the system undergoes a phase transition from the hadronic phase to the chiral restored and deconfined quark-gluon phase. In the case of physical quark masses, QCD chiral models as well as lattice QCD predict that the phase transition is a smooth crossover at small baryon chemical potential and high temperature [1–3]. Due to the sign problem, it is still quite challenging for lattice QCD simulation to work at finite baryon chemical potential. However, through symmetry class analysis [4, 5] and effective model predictions [6–23], it has been generally believed that the QCD phase transition is of first order at high baryon chemical potential, and the end point of the first order phase transition line toward the crossover region is called the critical end point (CEP). For theoretical reviews of the QCD phase diagram and the CEP, please refer to Refs. [24, 25] and references therein.

Different models, such as the Nambu–Jona-Lasinio (NJL) model, Polyakov-loop improved NJL (PNJL) model, linear sigma model, quark-meson (QM) model, Polyakov-loop improved QM model, and the Dyson-Schwinger equations (DSE), give various locations for

Received 3 July 2017, Revised 4 October 2017, Published online 17 November 2017

∗ Supported by NSFC (11275213, and 11261130311) (CRC 110 by DFG and NSFC), CAS key project KJCX2-EW-N01, and Youth Innovation Promotion Association of CAS

1) E-mail: lizb@ihep.ac.cn

2) E-mail: chenyd@ihep.ac.cn

3) E-mail: lidanning@jnu.edu.cn

4) E-mail: huangm@ihep.ac.cn

the CEP. Even the same model with different parameters can give different locations for the CEP [6–19]. Therefore, to search for the existence of the CEP and to locate the CEP in the QCD phase diagram is one of the most central goals at the Relativistic Heavy Ion Collider (RHIC), and it also sets a strong motivation for the future accelerator facilities at FAIR in Darmstadt and NICA in Dubna. In the first phase of the beam energy scan program (BES-I) by the STAR and PHENIX experiments at RHIC, which ran from 2010 to 2014, experimental measurements of the fluctuations of conserved quantities were performed for Au+Au collisions at $\sqrt{s_{\rm NN}}$ = 7.7,11.5,14.5,19.6,27,39,62.4 and 200 GeV. The experimental measurements of cumulants of conserved quantities up to the fourth order of net-proton, net-charge and net-kaon multiplicity distributions from BES-I [26, 27] are summarized in Ref. [28]. One interesting observation is that the kurtosis of the baryon number distributions $\kappa\sigma^2$ in the most central Au+Au collisions shows a non-monotonic energy dependence behavior. It decreases from almost 1 at the collision energy of $\sqrt{s_{\rm NN}}$=200 GeV to 0.1 at $\sqrt{s_{\rm NN}}$=20 GeV then starts to increase quickly to 3.5 at $\sqrt{s_{\rm NN}}$=7 GeV.

We are curious about whether the non-monotonic behavior of the kurtosis of the baryon number distributions is caused by the existence of the CEP. Furthermore, before the running of the second phase of the beam energy scan (BES-II) at RHIC in 2019-2020, it is urgent for theorists to offer a clean signature to identify the existence of the CEP, and even more to propose a method to locate the CEP. In this work, we are going to provide such an answer. It was shown in Ref. [21] that the quartic cumulant (or kurtosis) is universally negative when the critical point is approaching the crossover side of the phase separation line. Previously, much interest has focused on the decreasing and then increasing behavior of the kurtosis of the baryon number distributions around the collision energy $\sqrt{s_{\rm NN}}$ = 20 GeV, which is caused by the sign changing of various cumulants around the CEP. More sign changing for higher order susceptibilities has recently been discussed in Ref. [11], and it is found that for 6th and 8th order baryon number susceptibilities, the sign changing starts at the baryon chemical potential quite far away from the CEP.

In this work, we will show that the cumulant ratio (up to fourth order) of conserved number susceptibilities forms a ridge along the phase boundary on the $(T,\mu_{\rm B})$ plane, and if the CEP exists there, the conserved number susceptibility develops a high sharp hollow "mountain" or a sword-shaped "mountain" standing upright around the CEP, which is a model-independent universal feature. The measurement of number susceptibilities from heavy-ion collision experiments is along the freeze-out line, which is below the phase boundary. If the freeze-out line can cross the foot of the CEP mountain, then one is lucky enough to observe the peaked baryon number susceptibilities along the freeze-out line.

2 CEP from holographic QCD model and baryon number susceptibilities

In recent decades, a new nonperturbative method has been developed based on anti-de Sitter/conformal field theory (AdS/CFT) correspondence and the conjecture of gravity/gauge duality [29–31] to deal with strongly coupled QCD systems. In the framework of a holographic QCD (hQCD) model at finite baryon chemical potential, the CEP has been discussed in Refs. [32–35]. The model we use in this work is a simple hQCD model with the CEP located at higher baryon chemical potential, and the 5D Einstein-Maxwell-dilaton holographic model is described by the action [34]

$$S=\frac{1}{2\kappa_5^2}\int {\rm d}^5x\sqrt{-g}\left[R-\frac{f(\phi)}{4}F_{\mu\nu}^2-\frac{1}{2}(\partial\phi)^2-V(\phi)\right]. \quad (1)$$

The ansatz of the metric, Maxwell field and dilaton field are defined as [34]

$${\rm d}s^2=\frac{{\rm e}^{2A(z)}}{z^2}\left[-g(z){\rm d}t^2+\frac{1}{g(z)}{\rm d}z^2+{\rm d}\vec{x}^2\right], \quad (2)$$

and

$$\phi=\phi(z), \quad A_\mu=A_t(z), \quad (3)$$

with the regular boundary conditions at the horizon $z=z_{\rm H}$ and the asymptotic AdS_5 condition at the boundary $z=0$ [34]

$$A_t(z_{\rm H})=g(z_{\rm H})=0, \quad (4)$$

$$A(0)=-\sqrt{\frac{1}{6}}\phi(0), \quad g(0)=1, \quad (5)$$

$$A_t(0)=\mu+\rho z^2+\cdots, \quad (6)$$

where μ and ρ are the chemical potential and density of quarks respectively. The warp factor and gauge kinetic function can be fixed as [34]

$$A(z)=-\frac{c}{3}z^2-bz^4, \quad (7)$$

$$f(\phi(z))={\rm e}^{cz^2-A(z)}. \quad (8)$$

Then from the equation of motion we can calculate the quark density ρ and temperature T as

$$\rho=\frac{c\mu}{1-{\rm e}^{cz_{\rm H}^2}}, \quad (9)$$

$$T=\frac{z_{\rm H}^3{\rm e}^{-3A(z_{\rm H})}}{4\pi\int_0^{z_{\rm H}}y^3{\rm e}^{-3A(y)}{\rm d}y}\left[1-\frac{2c\mu^2}{(1-{\rm e}^{cz_{\rm H}^2})^2}\times\left({\rm e}^{cz_{\rm H}^2}\int_0^{z_{\rm H}}y^3{\rm e}^{-3A(y)}{\rm d}y-\int_0^{z_{\rm H}}y^3{\rm e}^{cy^2-3A(y)}{\rm d}y\right)\right]. \quad (10)$$

Here the parameters b and c are fixed from the meson spectrum and speed of sound [34] with $b=-6.25\times10^{-4}$ GeV^4, and $c=0.227$ GeV^2. Note that here we have fixed κ_5 to 1.

The entropy density s can be calculated as [33]

$$s=2\pi\frac{e^{3A(z_H)}}{z_H^3}, \tag{11}$$

then by using the free energy at fixed quark chemical potential [32, 34]

$$F=-\int sdT=-\int_{z_H}^{z_H(T_0)} s\frac{\partial T(z_H,\mu)}{\partial z_H}dz_H, \tag{12}$$

one can determine the phase structure of the model by minimizing the free energy. Here, the zero point of free energy is set at $T=T_0=170$ MeV. In the crossover region, the free energy is single valued at fixed μ as a function of T, while in the first order phase transition region, the free energy is multi-valued as a function of T at fixed μ. The critical temperature T_c for each μ and the location of the CEP are determined by minimizing the free energy at fixed μ. The phase structure of the holographic QCD model is shown in Fig. 1 with the CEP located at $(T^c,\mu_B^c)=(0.121$ GeV, 0.693 GeV), which is close to the CEP location given in Ref. [35]. The phase structure of this holographic QCD model, as well as that in Refs. [32, 33, 35], is for the deconfinement phase transition, and the CEP for the chiral phase transition in the holographic QCD model has not been realized yet. At the current stage, for simplicity we can assume that the chiral phase transition coincides with the deconfinement phase transition. In general, the chiral phase transition may be separate from the deconfinement phase transition, and work toward this goal in the framework of holographic QCD models in still in progress.

Using the parameterized relation between the collision energy $\sqrt{s_{NN}}$ and μ_B [36]

$$\mu_B(\sqrt{s_{NN}})=\frac{1.30}{1+0.28\sqrt{s_{NN}}}, \tag{13}$$

the corresponding collision energy at the CEP is $\sqrt{s_{NN}}=2.71$ GeV.

The measurements from heavy-ion collision experiment are along the freeze-out line, which should lie below the phase boundary. The purpose of our work is to investigate what kind of information about the CEP can be read from the measured baryon number fluctuations along the freeze-out line. Therefore, the distance between the freeze-out line and the phase boundary is essential. We choose three different cases: 1) the freeze-out line is close to the phase boundary and can cross the CEP mountain; 2) the freeze-out line can only cross the foot of the CEP mountain; and 3) the freeze-out line is far from the CEP region. These three chemical freeze-out lines are described by the following three polynomial fits:

$$f_i: T(\mu_B)=\alpha-\beta_i\mu_B^2-\gamma_i\mu_B^4 \quad i=1,2,3 \tag{14}$$

with $\alpha=0.145$, $\beta_1=0.040$, $\beta_2=0.060$, $\beta_3=0.160$, $\gamma_1=\gamma_2=0.040$, $\gamma_3=0.074$. The three chemical freeze-out lines f_1, f_2 and f_3 are shown in Fig. 1 by dashed, dashed-dotted and long dashed lines, respectively. The chemical freeze-out line f_1 is very close to the phase boundary, f_3 is away from the phase boundary, and f_2 is in between. In order to compare with experiment measurements, we choose that the system freezes out starting from ($T=145$ MeV,$\mu_B=0$) [37].

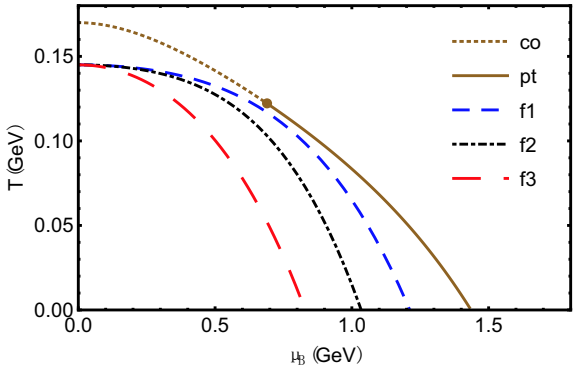

Fig. 1. (color online) The (T,μ_B) phase diagram in the 5D hQCD model. The brown dotted line is for the crossover, and the brown solid line is for the first order phase transition. The CEP is located at $(T^c,\mu_B^c)=(0.121$ GeV, 0.693 GeV). The blue dashed, black dashed-dotted, and the red long dashed lines represent the three chemical freeze-out conditions defined in Eq.(14).

The baryon number susceptibilities are defined as the derivative of the dimensionless pressure with respect to the reduced chemical potential [28]

$$\chi_n^B=\frac{\partial^n[P/T^4]}{\partial[\mu_B/T]^n} \tag{15}$$

with the pressure $P=-F$ just the negative free energy [33]. The cumulants of baryon number distributions are given by

$$C_n^B=VT^3\chi_n^B \tag{16}$$

Introducing the mean $M=C_1^B$, variance $\sigma^2=C_2^B$, skewness $S=\frac{C_3^B}{(\sigma^2)^{3/2}}$ and kurtosis $\kappa=\frac{C_4^B}{(\sigma^2)^2}$, one can have the following relations between observable quantities and theoretical calculations

$$\begin{aligned}\frac{\sigma^2}{M}&=\frac{C_2^B}{C_1^B}=\frac{\chi_2^B}{\chi_1^B}, \quad S\sigma=\frac{C_3^B}{C_2^B}=\frac{\chi_3^B}{\chi_2^B},\\ \frac{S\sigma^3}{M}&=\frac{C_3^B}{C_1^B}=\frac{\chi_3^B}{\chi_1^B}, \quad \kappa\sigma^2=\frac{C_4^B}{C_2^B}=\frac{\chi_4^B}{\chi_2^B}.\end{aligned} \tag{17}$$

3 Numerical results

Figure 2 shows a 3-dimensional plot of σ^2/M, $S\sigma$, $S\sigma^3/M$, and $\kappa\sigma^2$ as functions of the temperature T and the baryon chemical potential $\mu_{\rm B}$. Each ratio of the baryon number susceptibilities σ^2/M, $S\sigma$, $S\sigma^3/M$, and $\kappa\sigma^2$ forms an obvious ridge along the phase boundary, and it develops a high sharp hollow sword-shaped mountain standing upright around the CEP in a narrow oblate region. The CEP mountains are hollow because these ratios of the baryon number susceptibilities are negative inside this oblate region [21]. The ridge profile along the phase boundary and the sword-shaped CEP mountain for baryon number susceptibilities (up to fourth order) are universal features for phase transitions and the existence of CEP, respectively [8–10, 35]. The magnitude of the cumulant ratios of baryon number fluctuations (up to fourth order) decreases with the increase of the baryon chemical potential along the phase boundary, and the competition between the decreasing tendency of the ridge and the rising of the hollow CEP mountain determines the shape of the baryon number fluctuations along the phase boundary or freeze-out line. However, the height of the ridge along the phase boundary or the magnitude of the cumulant ratios at $\mu_{\rm B}=0$, and the location of the CEP, are model-dependent, so in different models, we see different negative region for kurtosis, and different profiles of the cumulant ratios along the freeze-out line. We will explain this in more detail by using a different effective model in a coming paper [38].

The baryon number susceptibilities σ^2/M, $S\sigma$, $S\sigma^3/M$, and $\kappa\sigma^2$ along the three chemical freeze-out lines f_1, f_2 and f_3 are also shown in Fig. 2 by dashed, dashed-dotted and long dashed lines, respectively. If the freeze-out line is very close to the phase boundary, as for f_1, it climbs up to the sword mountain of the CEP a little bit, and the ratios of the baryon number susceptibilities σ^2/M, $S\sigma$, $S\sigma^3/M$, and $\kappa\sigma^2$ show high peaks along the freeze-out line. If the freeze-out line is away from the phase boundary, as for f_3, it crosses the flat plane, and almost all the ratios of the baryon number susceptibilities of σ^2/M, $S\sigma$, $S\sigma^3/M$, and $\kappa\sigma^2$ show a monotonic decreasing behavior along the freeze-out line, except for $S\sigma$. If the freeze-out line is not far away from the phase boundary, as for f_2, and it can cross the foot of the sword mountain of the CEP, the ratios of the baryon number susceptibilities σ^2/M, $S\sigma$, $S\sigma^3/M$, and $\kappa\sigma^2$ show obvious peaks along the freeze-out line. The closer the freeze-out line to the phase boundary, the higher the peak of the number susceptibilities. Among the four ratios of the baryon number susceptibilities σ^2/M, $S\sigma$, $S\sigma^3/M$, and $\kappa\sigma^2$, it is found that the peak of the kurtosis $\kappa\sigma^2$ has the tallest magnitude for the same freeze-out condition.

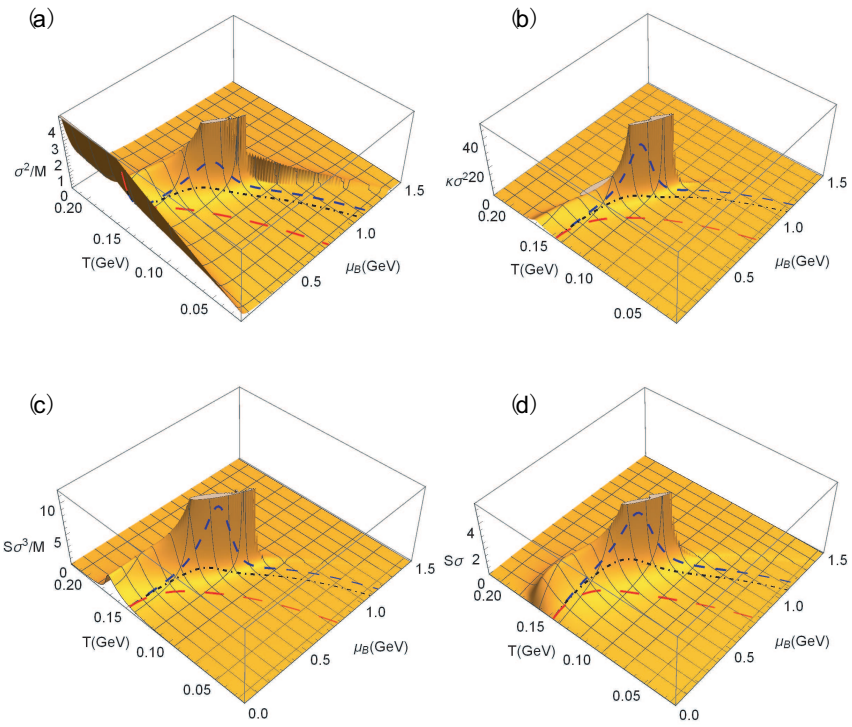

Fig. 2. (color online) 3D plot of σ^2/M, $S\sigma$, $S\sigma^3/M$, $\kappa\sigma^2$ as functions of the temperature T and the baryon chemical potential $\mu_{\rm B}$. The blue dashed, black dashed-dotted, and the red long dashed lines represent the three chemical freeze-out conditions defined in Eq.(14).

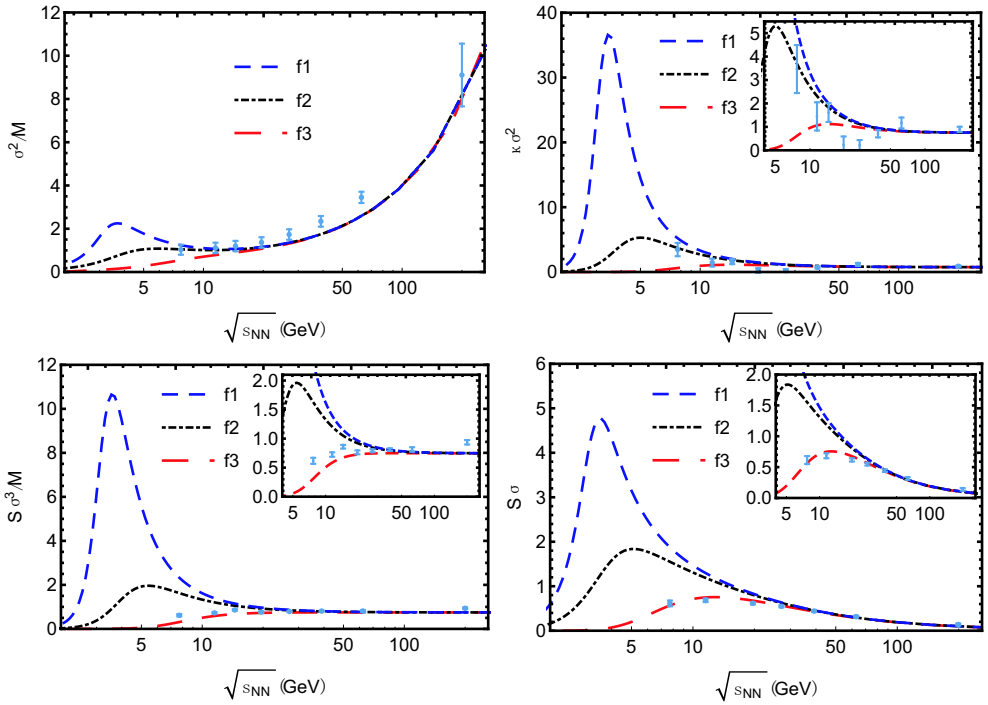

Fig. 3. (color online) σ^2/M, $S\sigma$, $S\sigma^3/M$, $\kappa\sigma^2$ along freeze-out lines as a function of the collision energy $\sqrt{s_{\rm NN}}$ and compared with experimental measurements. The blue dashed, black dashed-dotted, and the red long dashed lines represent the three chemical freeze-out conditions defined in Eq.(14).

In Fig. 3, we compare our model results with experimental measurements of the baryon number susceptibilities σ^2/M, $S\sigma$, $S\sigma^3/M$, and $\kappa\sigma^2$ along the three freeze-out lines f_1, f_2 and f_3 as a function of the collision energy $\sqrt{s_{\rm NN}}$. Above the collision energy of $\sqrt{s_{\rm NN}} = 20$ GeV, the model results along all three freeze-out lines are in very good agreement with the experimental results. The experimental measurements of even cumulants σ^2/M ($C_2^{\rm B}/C_1^{\rm B}$) and $\kappa\sigma^2$ ($C_4^{\rm B}/C_2^{\rm B}$) follow the freeze-out line f_2, while experimental measurements of the odd cumulants $S\sigma^3/M$ ($C_3^{\rm B}/C_1^{\rm B}$) and $S\sigma(C_3^{\rm B}/C_2^{\rm B})$ go along the freeze-out line f_3. One natural reason might be that different bases are chosen for odd and even cumulant ratios during experimental data analysis [28, 39]. However, it might be caused by other reasons, e.g. only protons are measured in the experiment, or due to non-thermal effects, or memory effects [40]. This deserves further study in the future.

Because higher cumulants have higher magnitude around the CEP, we focus only on the kurtosis measurement $\kappa\sigma^2$. The measurement of $\kappa\sigma^2$ follows the freeze-out line f_2, and the current data indicate that it should show a peak around the collision energy $\sqrt{s_{\rm NN}}=5$ GeV. As we have explained above, because the freeze-out line f_2 is close to the phase boundary, and crosses the foot of the CEP mountain, one can observe an obvious peak of the baryon number susceptibilities along the freeze-out line. The peaked kurtosis $\kappa\sigma^2$ along the freeze-out line gives an evident signature of the existence of the CEP, and we can estimate that the CEP is located nearby, around the collision energy $\sqrt{s_{\rm NN}}=3-7$ GeV. Also, for the experimental data the kurtosis shows a dip near collision energies of 19.6 and 27 GeV, while the kurtosis in the current holographic QCD model does not have a dip. As we have pointed out, the fine structure of the baryon number fluctuations along the freeze-out line is determined by the competition between the decreasing tendency of the ridge of phase transition and the rising of the hollow CEP mountain. We will analyze this part in detail in a coming paper by using a different model. The fine structure of the cumulant ratio along the freeze-out line is model-dependent. Only the peak structure along the freeze-out line for kurtosis is caused by the CEP itself, and thus it can be regarded as a clean signature for the existence of the CEP.

4 Discussion and conclusions

In summary, we have explained why the peaked baryon number susceptibilities, especially the kurtosis $\kappa\sigma^2$, along the freeze-out line can be used as an evident signature for the existence of the CEP. The peak position can also be used to locate the approximate region of the CEP in the QCD phase diagram. If the CEP exists, a universal feature of the 3D profile of baryon number susceptibilities (up to fourth order) is that it forms a ridge

along the phase boundary and develops a sword-shaped mountain standing upright around the CEP in a narrow oblate region. The magnitude of the cumulant ratios of baryon number fluctuations (up to fourth order) has tends to decrease with increasing baryon chemical potential along the phase boundary, and the competition between the decreasing tendency of the ridge and the rising of the hollow CEP mountain determines the shape of the baryon number fluctuations along the phase boundary or freeze-out line. The height of the ridge along the phase boundary and the location of the CEP are model-dependent. Therefore we would like to emphasize that the fine structure of the cumulant ratio along the freeze-out line is model-dependent. Only the peak structure along the freeze-out line for kurtosis is caused by the CEP itself, and thus it can be regarded as a clean signature for the existence of the CEP. The sword-shaped CEP mountain stands on the $(T,\mu_{\rm B})$ plane in a very narrow and oblate region along the phase boundary, and the foot area is also quite narrow and oblate. Therefore, if we can observe the peaked kurtosis $\kappa\sigma^2$ along the freeze-out line, this means that the real freeze-out line can cross the narrow foot of the CEP mountain. That would be very advantageous for experimentalists! Our analysis estimates that the peak of the kurtosis $\kappa\sigma^2$ would show up around the collision energy $\sqrt{s_{\rm NN}}$=5 GeV, and the CEP would be located around the collision energy $\sqrt{s_{\rm NN}}$=3–7 GeV. If the finite size effect is taken into account, it might broaden the CEP region a little bit, and it would give more chances for experimentalists to find the CEP. Finally, the universal feature observed around the CEP should also apply to the case of the first-order liquid-gas phase transition for nuclear matter, which is located at a rather low temperature ($T_{\rm c}$=19.7 MeV, $\mu_{\rm B}^{\rm c}$= 908 MeV) [41]. If the freeze-out line crosses the feet of two CEP mountains, one may observe two peaks for the baryon number susceptibilities, while if the freeze-out line crosses the ridge of the liquid-gas phase transition as shown in Ref. [41], the baryon number susceptibilities will become very negative when approaching the CEP and then sharply rise when crossing the CEP of the liquid-gap phase transition.

We thank X.F.Luo, I.Shovkovy, and H. Stoecker for valuable discussions.

References

1 Z. Fodor and S. D. Katz, Phys. Lett. B, **534**: 87 (2002)
2 H. T. Ding, F. Karsch, and S. Mukherjee, Int. J. Mod. Phys. E, **24**(10): 1530007 (2015) doi:10.1142/S0218301315300076 [arXiv:1504.05274 [hep-lat]]
3 C. Schmidt and S. Sharma, arXiv:1701.04707 [hep-lat]
4 R. D. Pisarski and F. Wilczek, Phys. Rev. D, **29**: 338 (1984)
5 Y. Hatta and T. Ikeda, Phys. Rev. D, **67**: 014028 (2003)
6 T. M. Schwarz, S. P. Klevansky, and G. Papp, Phys. Rev. C, **60**: 055205 (1999)
7 P. Zhuang, M. Huang, and Z. Yang, Phys. Rev. C, **62**: 054901 (2000)
8 J. W. Chen, J. Deng, and L. Labun, Phys. Rev. D, **92**(5): 054019 (2015)
9 J. W. Chen, J. Deng, H. Kohyama, and L. Labun, Phys. Rev. D, **93**(3): 034037 (2016)
10 W. Fan, X. Luo, and H. S. Zong, Int. J. Mod. Phys. A, **32**(11): 1750061 (2017)
11 W. Fan, X. Luo, and H. Zong, arXiv:1702.08674 [hep-ph]
12 W. j. Fu and Y. l. Wu, Phys. Rev. D, **82**: 074013 (2010)
13 E. S. Bowman and J. I. Kapusta, Phys. Rev. C, **79**: 015202 (2009)
14 H. Mao, J. Jin, and M. Huang, J. Phys. G, **37**: 035001 (2010)
15 B. J. Schaefer and M. Wagner, Phys. Rev. D, **85**: 034027 (2012)
16 B. J. Schaefer and M. Wagner, Central Eur. J. Phys., **10**: 1326 (2012)
17 S. x. Qin, L. Chang, H. Chen, Y. x. Liu, and C. D. Roberts, Phys. Rev. Lett., **106**: 172301 (2011)
18 J. Luecker, C. S. Fischer, L. Fister, and J. M. Pawlowski, PoS CPOD, **2013**: 057 (2013)
19 W. j. Fu, J. M. Pawlowski, F. Rennecke, and B. J. Schaefer, Phys. Rev. D, **94**(11): 116020 (2016)
20 M. A. Stephanov, Phys. Rev. Lett., **102**: 032301 (2009)
21 M. A. Stephanov, Phys. Rev. Lett., **107**: 052301 (2011)
22 M. Asakawa, S. Ejiri, and M. Kitazawa, Phys. Rev. Lett., **103**: 262301 (2009)
23 C. Athanasiou, K. Rajagopal, and M. Stephanov, Phys. Rev. D, **82**: 074008 (2010)
24 M. A. Stephanov, Prog. Theor. Phys. Suppl., **153**: 139 (2004); Int. J. Mod. Phys. A, **20**: 4387 (2005)
25 M. A. Stephanov, PoS LAT, **2006**: 024 (2006)
26 L. Adamczyk et al (STAR Collaboration), Phys. Rev. Lett., **112**: 032302 (2014)
27 M. M. Aggarwal et al (STAR Collaboration), Phys. Rev. Lett., **105**: 022302 (2010)
28 X. Luo and N. Xu, arXiv:1701.02105 [nucl-ex]
29 J. M. Maldacena, Adv. Theor. Math. Phys., **2**: 231 (1998); Int. J. Theor. Phys., **38**: 1113 (1999)
30 S. S. Gubser, I. R. Klebanov, and A. M. Polyakov, Phys. Lett. B, **428**: 105 (1998)
31 E. Witten, Adv. Theor. Math. Phys., **2**: 253 (1998)
32 O. DeWolfe, S. S. Gubser, and C. Rosen, Phys. Rev. D, **83**: 086005 (2011)
33 O. DeWolfe, S. S. Gubser, and C. Rosen, Phys. Rev. D, **84**: 126014 (2011)
34 Y. Yang and P. H. Yuan, JHEP, **1411**: 149 (2014)
35 R. Critelli, J. Noronha, J. Noronha-Hostler, I. Portillo, C. Ratti, and R. Rougemont, arXiv:1706.00455 [nucl-th]
36 A. Kadeer, J. G. Korner, and U. Moosbrugger, Eur. Phys. J. C, **59**: 27 (2009)
37 S. Borsanyi, Z. Fodor, S. D. Katz, S. Krieg, C. Ratti, and K. K. Szabo, Phys. Rev. Lett., **113**: 052301 (2014); A. Bazavov et al, Phys. Rev. D, **93**(1): 014512 (2016);
38 Z. B. Li, X. Y. Wang, and M. Huang, in preparation
39 We thank discussion with X.F. Luo on this point
40 S. Mukherjee, R. Venugopalan, and Y. Yin, Phys. Rev. C, **92**(3): 034912 (2015); S. Mukherjee, R. Venugopalan, and Y. Yin, Phys. Rev. Lett., **117**(22): 222301 (2016); L. Jiang, P. Li, and H. Song, Phys. Rev. C, **94**(2): 024918 (2016)
41 V. Vovchenko, M. I. Gorenstein, and H. Stoecker, Phys. Rev. Lett., **118**(18): 182301 (2017)